

Perturbative studies of electron transport in NSTX

D. Stutman¹, K. Tritz¹, L. Delgado¹, M. Finkenthal¹, M. Bell², R. Bell², C. Bush³, S. Kaye²,
H. Kugel², B. LeBlanc², R. Maingi³, V. Soukhanovskii⁴

¹ *Johns Hopkins University, Baltimore, USA*

² *Princeton Plasma Physics Laboratory, Princeton, USA*

³ *Oak Ridge National Laboratory, Oak Ridge, USA*

⁴ *Lawrence Livermore National Laboratory, Livermore, USA*

Abstract

The study of electron transport is important for an understanding of present machines and predicting performance in future machines, such as ITER. NSTX provides a unique test bed for probing electron transport due to its dominant role in the overall power balance [1]. Global T_e profile crashes of 10-25% amplitude are observed following large Type I ELMs in some beam heated H-mode NSTX discharges. While the SXR imaging indicates that the ELM itself is causing only a peripheral MHD perturbation, the propagation of the cold pulse initiated by the ELM is unusually fast (ms time scale) and can extend to the core of the plasma. The perturbed electron thermal diffusivity is estimated to be in the hundred m^2/s range in the outer plasma, decreasing towards the centre. Motivated by these observations, we produced also controlled perturbations at the plasma edge by injecting small low-Z pellets into beam heated H-mode plasmas, and compared the ELM and pellet induced cold pulse using two-colour SXR imaging. In plasmas which exhibit large Type I ELMs the pellet perturbation has a similarly large effect on the global T_e profile, with a stiff behaviour of the core profile. In contrast, the particle diffusivity estimated from the decay of pellet injected impurity is in the m^2/s range. The about two order of magnitude difference suggests magnetic effects in the perturbed NSTX electron transport.

Experiment

Small (≈ 0.5 mg) Li pellets were injected into double null diverted H-mode discharges, using a low velocity (≈ 100 m/s) pellet injector. The base line discharges had $I_p=0.8-1$ MA, $B_t=4.5$ kG, $\kappa \approx 2$, $\delta \approx 0.6$, and were heated by 6 MW of deuterium beam injection at 100 keV. Fast imaging with visible cameras filtered for neutral Li lines shows

strong emission on peripheral field lines, indicating that the pellet ablates in the plasma edge (Fig. 1a). The T_e and n_e profiles measured by the NSTX Multi Point Thomson Scattering system, MPTS, about 3 ms before and 2 ms after the pellet ablation at the edge, are shown in Fig. 1b. As seen, the edge perturbation causes a $\approx 20\%$ global drop in the T_e profile, which leaves essentially unchanged the normalized gradient, R/L_{T_e} . At the same time, the electron density is nearly unperturbed, with only a several percent increase in the pedestal region, which further confirms the shallow pellet penetration. The magnetic diagnostics indicate also that the plasma position and shape are little perturbed.

To determine how the T_e profile evolves in between the MPTS time points in these experiments, we used a ‘two-colour’ SXR technique [2], based on simultaneously imaging the plasma with filtered diode arrays having 0.6 keV and 1.4 keV cut off energies (Fig. 2). The evolution of the two-colour SXR profiles around the time of the pellet impact is shown in Fig. 3, together with a trace of the Li III 135 Å emission from the pellet, measured by a multilayer mirror telescope. The $E > 0.6$ keV emission, which is weighted towards the cooler edge, shows an almost instantaneous crash at the pellet arrival. The $E > 1.4$ keV emission, which is weighted towards the hotter core, shows a subsequent cold pulse propagating to the centre on ms time scale.

The evolution of the T_e profile during the perturbation is obtained by modelling the ratio of the $E > 1.4$ keV to $E > 0.6$ keV emission profiles, as discussed in Ref. 2. The computation starts from the MPTS T_e profile before the perturbation and the subsequent profiles are obtained through a fit in which the T_e profile is let to vary and the small n_e , n_z perturbation neglected. The validity of the technique is confirmed by the agreement between the next MPTS T_e profile after perturbation and that predicted by SXR modelling.

The characteristic cold pulse evolution is illustrated in Fig. 4 through a plot of the normalized T_e gradient during the perturbation. This confirms that the temperature evolves with little gradient change in the core (‘stiff’ transport), as suggested by the MPTS profiles in Fig. 1. A larger gradient change is computed in the peripheral region. There however the SXR calculation has a larger error, due to some high-Z impurity content in these plasmas.

A similar picture is observed following edge T_e perturbations induced by large Type-I ELMs. This is illustrated by the two-colour SXR profiles in Fig. 5. As shown in Fig. 5a, the ELM perturbation occurs on the MHD time scale of a few tens of μ s and is restricted to the outermost SXR chords (a few cm inside the separatrix). The cold pulse initiated by the ELM propagates to the centre however on the same ms time scale as for

pellet perturbations. Due to the absence of high-Z impurities, the cold pulse analysis was more accurate in this case, enabling an estimate of the perturbed χ_e from the core to the peripheral plasma. The values obtained using either a simple time-to-peak calculation [3], or the more involved cold pulse model as in Ref. 4, range from tens of m^2/s in the inner plasma, to hundreds of m^2/s in the outer region. This is consistent with the cold pulse reaching the centre on ms time scale, over a minor radius of ≈ 0.8 m in NSTX.

This unusually fast propagation of the T_e perturbation raises the fundamental question if long wavelength electrostatic turbulence can produce such rapid electron transport. To try and shed some light we used pellet injection to estimate also the local particle transport in these plasmas. 0.5 mg pellets of vitreous C (a glassy, ablation resistant material) were injected in the above H-mode discharges and the evolution of the pellet deposited C ions measured by the charge-exchange recombination spectroscopy diagnostic (CHERS). The glassy C pellet enabled deeper penetration and created a transient density of C ions in the outer plasma (Fig. 6a). As seen in Fig. 6a, the particle perturbation decays on a much longer time scale than that involved in the electron thermal perturbation. The evolution of this perturbation was simulated with the MIST impurity transport code, as shown in Fig. 6b. A good match obtains for the diffusivity profile in Fig. 6c, which has D_C around $1 \text{ m}^2/\text{s}$ in the outer plasma. This value is in the neoclassical range for NSTX [5] and about two orders of magnitude lower the estimated perturbative χ_e . The thermal ion transport in these plasmas is also in the neoclassical range [1]. This large disparity between particle transport and electron thermal transport seems to preclude long wavelength electrostatic turbulence as a cause for the rapid perturbed electron transport in NSTX. While short wavelength electrostatic turbulence could be invoked, a simpler explanation may be that magnetic effects are present. Indeed, the diffusivity of test particles moving along a stochastic field scales as $D_i \approx \chi_i \approx \chi_e (m_e/m_i)^{1/2}$ [6]. This would give about two orders of magnitude difference between the electron thermal and the C particle transport, consistent with the observations.

Finally, we note that the close similarity between pellet and Type-I ELM induced temperature perturbations observed in NSTX seems to suggest a closer relation between Type-I ELMs and perturbed electron transport than generally considered. This aspect could also be important for future reactors such as ITER.

[1] S. Kaye et al., *Nucl. Fusion* **45**, S168 (2005)

[2] D. Stutman et al., *Rev. Sci. Instrum.* **74**, 1982 (2003)

- [3] L. Cardoso, *Plasma Phys. Control. Fusion* **37**, 799 (1995)
 [4] S. Inagaki et al., *Plasma Phys. Control. Fusion* **46**, A71-A76 (2004)
 [5] D. Stutman et al., *Phys. Plasmas* **10**, 4387 (2003)
 [6] J. Connor, *Plasma Phys. Control. Fusion* **35**, B293 (1993)

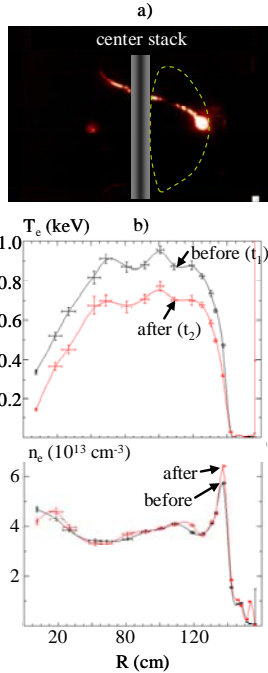


Fig. 1 a) Li I light image of ablation of 0.5 mg Li pellet in 1 MA, 6 MW NSTX H-mode. b) Thomson scattering profiles 3 ms before and 2 ms after pellet arrival.

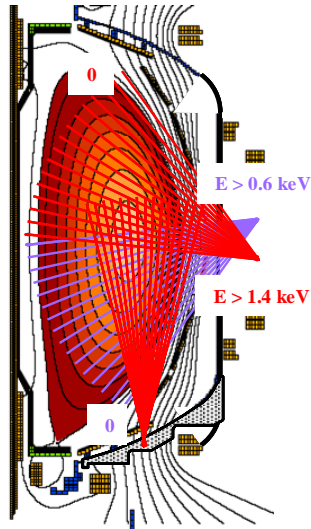


Fig. 2 Layout of two-color SXR system on NSTX. Chords 0 view the edge.

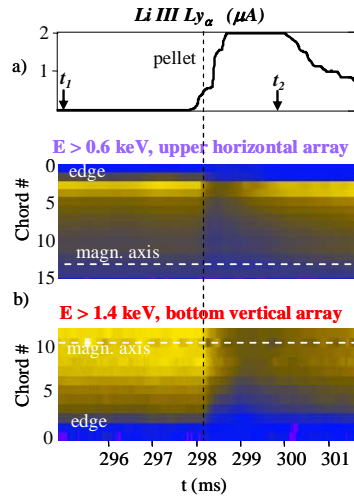


Fig. 3 a) Trace of Li III Ly α emitted by the pellet. Also indicated the MPTS time points from Fig. 1 b) Intensity plot of 'two-color' SXR data

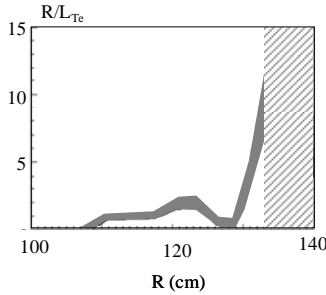


Fig. 4 Normalized T_e gradient during pellet cold pulse propagation computed using the two-color SXR data. The plot covers a 4 ms interval, starting 1 ms before pellet arrival.

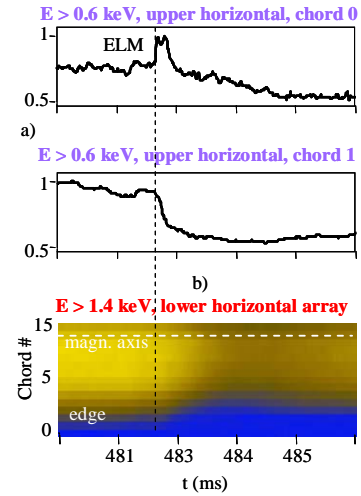


Fig. 5 a) Traces of edge SXR emission at Type-I ELM in 0.8 MA, 6 MW H-mode. Chord 1 views the plasma at $\rho \approx 0.8-0.9$. b) Intensity plot of core SXR emission

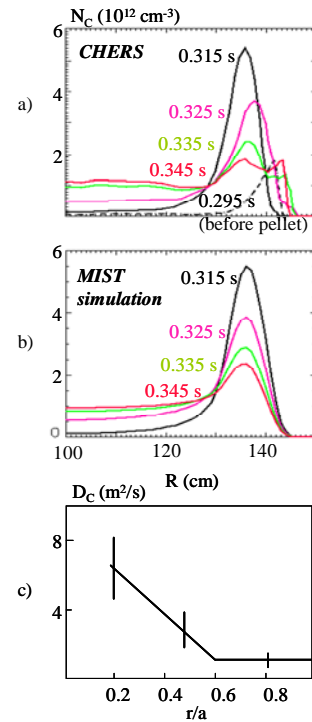


Fig. 6 a) Decay of C density perturbation following injection of 0.5 mg vitreous C in 1 MA, 6 MW H-mode. b) MIST simulation of the injection c) Diffusivity profile used in the MIST simulation. An outward convective velocity of a few m/s is also necessary to reproduce the data.